Runaway electron generation as possible trigger for enhancement of magnetohydrodynamic plasma activity and fast changes in runaway beam behavior

I. M. Pankratov, R. J. Zhou, and L. Q. Hu

Citation: Physics of Plasmas **22**, 072115 (2015); doi: 10.1063/1.4927578
View online: http://dx.doi.org/10.1063/1.4927578
View Table of Contents: http://scitation.aip.org/content/aip/journal/pop/22/7?ver=pdfcov
Published by the AIP Publishing

Runaway electron generation as possible trigger for enhancement of magnetohydrodynamic plasma activity and fast changes in runaway beam behavior

I. M. Pankratov,[1,a)] R. J. Zhou,[2,a)] and L. Q. Hu[2]
[1]*Institute of Plasma Physics, NSC Kharkov Institute of Physics and Technology, Academicheskaya Str. 1, 61108 Kharkov, Ukraine*
[2]*Institute of Plasma Physics, Chinese Academy of Sciences, Hefei 230031, China*

(Received 13 March 2015; accepted 3 July 2015; published online 29 July 2015)

Peculiar phenomena were observed during experiments with runaway electrons: rapid changes in the synchrotron spot and its intensity that coincided with stepwise increases in the electron cyclotron emission (ECE) signal (cyclotron radiation of suprathermal electrons). These phenomena were initially observed in TEXTOR (Tokamak Experiment for Technology Oriented Research), where these events only occurred in the current decay phase or in discharges with thin stable runaway beams at a $q = 1$ drift surface. These rapid changes in the synchrotron spot were interpreted by the TEXTOR team as a fast pitch angle scattering event. Recently, similar rapid changes in the synchrotron spot and its intensity that coincided with stepwise increases in the non-thermal ECE signal were observed in the EAST (Experimental Advanced Superconducting Tokamak) runaway discharge. Runaway electrons were located around the $q = 2$ rational magnetic surface (ring-like runaway electron beam). During the EAST runaway discharge, stepwise ECE signal increases coincided with enhanced magnetohydrodynamic (MHD) activity. This behavior was peculiar to this shot. In this paper, we show that these non-thermal ECE step-like jumps were related to the abrupt growth of suprathermal electrons induced by bursting electric fields at reconnection events during this MHD plasma activity. Enhancement of the secondary runaway electron generation also occurred simultaneously. Local changes in the current-density gradient appeared because of local enhancement of the runaway electron generation process. These current-density gradient changes are considered to be a possible trigger for enhancement of the MHD plasma activity and the rapid changes in runaway beam behavior. © *2015 AIP Publishing LLC*.
[http://dx.doi.org/10.1063/1.4927578]

I. INTRODUCTION

Generation of runaway electrons during disruptions poses a potential threat to the safe operation of large tokamaks, and especially to ITER. The energies of runaway electrons can reach as high as tens of MeV. These runaway electrons can cause serious damage to plasma-facing-component surfaces.[1,2] At the same time, runaway electron generation is a fundamental physical phenomenon. Runaway electrons are generated when the electron energy exceeds a critical energy at which the electric field driving force on the electrons is equal to the minimum frictional drag force in the plasma. There are primary generation (Dreicer generation[3]) and secondary generation (avalanche generation[4]) processes.

During experiments with runaway electrons, peculiar events have been discovered: rapid changes in the synchrotron spot and its intensity that coincide with stepwise increases in the electron cyclotron emission (ECE) signal (the cyclotron radiation of suprathermal electrons). These phenomena were initially observed in TEXTOR (Tokamak Experiment for Technology Oriented Research), where these events only occurred in the current decay phase or in discharges with thin stable runaway beams at the $q = 1$ drift surface.[5,6]

It was observed that the synchrotron spot intensity can change with changes in the energy of the runaways, the number of runaways, or the pitch angle.[5] Because of the short time scales of these events, it was concluded that fast pitch angle scattering was the only possible explanation. On the basis of these arguments, the rapid changes in the synchrotron spot were interpreted by the TEXTOR team as being a fast pitch angle scattering (FPAS) event. They concluded that this event does not affect the bulk plasma. In the majority of cases, the TEXTOR neutron signal (the result of photonuclear reactions when the high energy runaway electrons strike the plasma facing materials) showed no change at all during FPAS, and peaks in the neutron signal only appeared occasionally during FPAS. No large runaway electron losses occurred during the FPAS events in TEXTOR. However, magnetic mode activity was often observed in these TEXTOR shots, and shots with FPAS events sometimes showed small modulations of the synchrotron spot before the FPAS event that acted as an indication of mode activity. It was also hypothesized that these phenomena were related to the value of the effective ion charge number Z_{eff}. The increase in the perpendicular energy of the runaways was not recognized in diamagnetic measurements because the number of runaways in TEXTOR was too small.

[a)]Authors to whom correspondence should be addressed. Electronic addresses: pankratov@kipt.kharkov.ua and rjzhou@ipp.ac.cn

Recently, rapid changes in the synchrotron spot and its intensity that coincided with stepwise ECE increases were observed in the Experimental Advanced Superconducting Tokamak (EAST) runaway discharge #28957.[7] In Ref. 7, these rapid changes in the synchrotron spot and their correlation with stepwise ECE increases were interpreted (as they were by the TEXTOR team) as FPAS events.

In this paper, we show that the step-like jumps in the ECE signal were connected to abrupt growth in the suprathermal electrons induced by bursting electric fields at reconnection events during magnetohydrodynamic (MHD) plasma activity.[8] At the same time, the runaway (non-thermal) electron generation is considered as a possible trigger for enhancement of MHD plasma activity and for the rapid changes in runaway beam behavior.

In the Introduction, the TEXTOR experimental results of rapid changes in synchrotron spot and intensity, and their coincidence with ECE signal stepwise increases are presented. The rest of this paper is organized as follows. Section II describes the experimental setup and the diagnostics of EAST. In Section III, we describe the EAST experiments, in which the interrelation between the enhanced MHD plasma activity, the stepwise increases in the ECE signals, and the rapid changes in the synchrotron spot (change in the IR spot from a hollow structure to a filled structure) are observed. In Section IV, the interpretations of these EAST experiments are discussed. Our conclusions are given in Section V.

II. EXPERIMENTAL SETUP AND DIAGNOSTICS

The investigated discharge in EAST was ohmic discharge #28957 (Figure 1) and was performed in the limiter configuration, with the toroidal magnetic field $B_0 = 2\,\mathrm{T}$, the plasma current $I_\mathrm{p} = 250\,\mathrm{kA}$, the central line-averaged density $\langle n_\mathrm{e} \rangle = 2.2 \times 10^{19}\,\mathrm{m}^{-3}$, the plasma major radius $R = 1.86\,\mathrm{m}$, and the minor radius $a = 0.45\,\mathrm{m}$.[7] At the plasma center, the electron temperature $T_\mathrm{e} \approx 0.55\,\mathrm{keV}$ was obtained using a soft x-ray pulse height analysis (PHA) system during the plasma current flat-top phase. MHD modes $m/n = 1/1$ (the soft x-ray signal) and $m/n = 2/1$ (the Mirnov coil signals) existed in the plasma, where m and n are the poloidal and toroidal mode numbers.

Runaway electrons were created by the ohmic coil during the start-up phase of the discharge. The runaway electrons were located around the $q = 2$ rational magnetic surface (ring-like runaway electron beam).[7,9] Approximately, 46% of the plasma current was carried by the runaways.[7] Under these conditions, the ECE signals were dominated by the runaway electrons in an energy range of approximately 0.3 MeV–3 MeV and could not represent the electron temperature. This is why we used the soft x-ray PHA system to obtain the electron temperature, rather than the ECE signals. The fact that the electron temperature given by the soft x-ray PHA is much lower than that given by the ECE measurements indicates again that the behavior of ECE signals was affected and was dominated by the runaway electrons in the discharge. In Fig. 1, the signals of the ECE02–ECE08 channels are shown. The signal of the ECE01 channel was saturated. The ECE system detected the emission of electrons from the beginning of the runaway region (suprathermal electrons). The step-like non-thermal ECE jumps in the ECE02–ECE05 channels are visible. The ECE08 channel should receive the second harmonic X-mode ECE of the thermal electrons at the center of the plasma and the ECE02 channel should receive the emission of the thermal electrons from the low-field side.

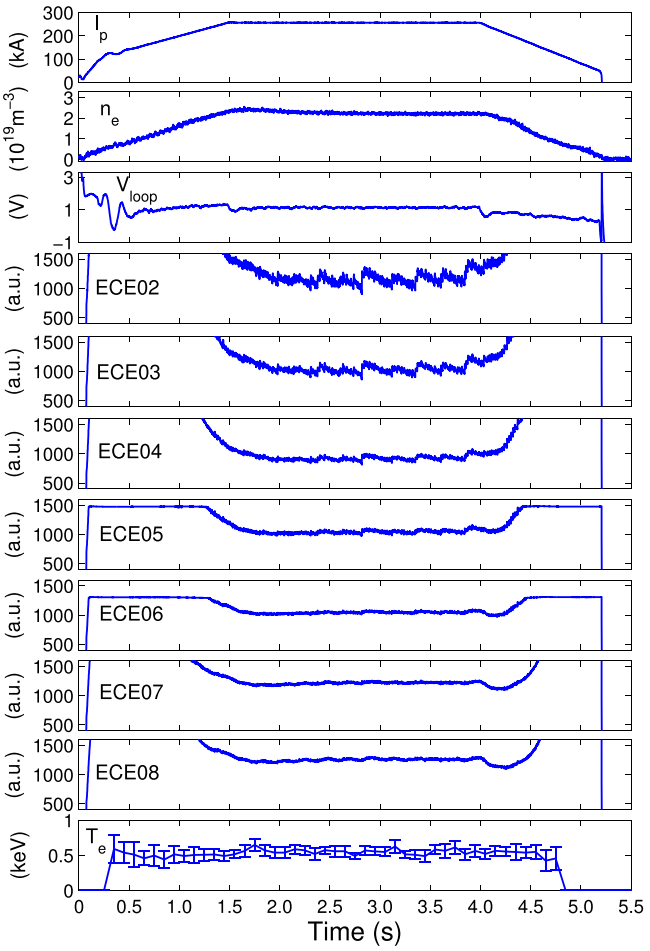

FIG. 1. Time slice of runaway discharge #28957: plasma current I_p, central line-averaged density, loop voltage V_loop, non-thermal ECE signals, and electron temperature at the plasma center taken from the soft x-ray PHA system.

The synchrotron radiation that originated from the energetic runaway electrons was measured using two visible light cameras.[7,10] One black and white camera was positioned in the direction of the electron approach on the equatorial plane and can measure synchrotron radiation in the 380–750 nm wavelength range, and one color camera was positioned in the direction opposite to the electron approach. The difference between the images given by these two cameras indicated that the bright ring-like structure originated from the runaway electron beam that was confined in the plasma.[7]

The hard x-ray was detected using a bismuth germanate (BGO) scintillator detector. This detector was installed outside the tokamak and was dedicated to measure thick-target bremsstrahlung emission in the 0.5–10 MeV energy range that was caused by runaway electrons when they were lost and struck the limiter or vessel structures. The signal from the neutron detector did not change at all.

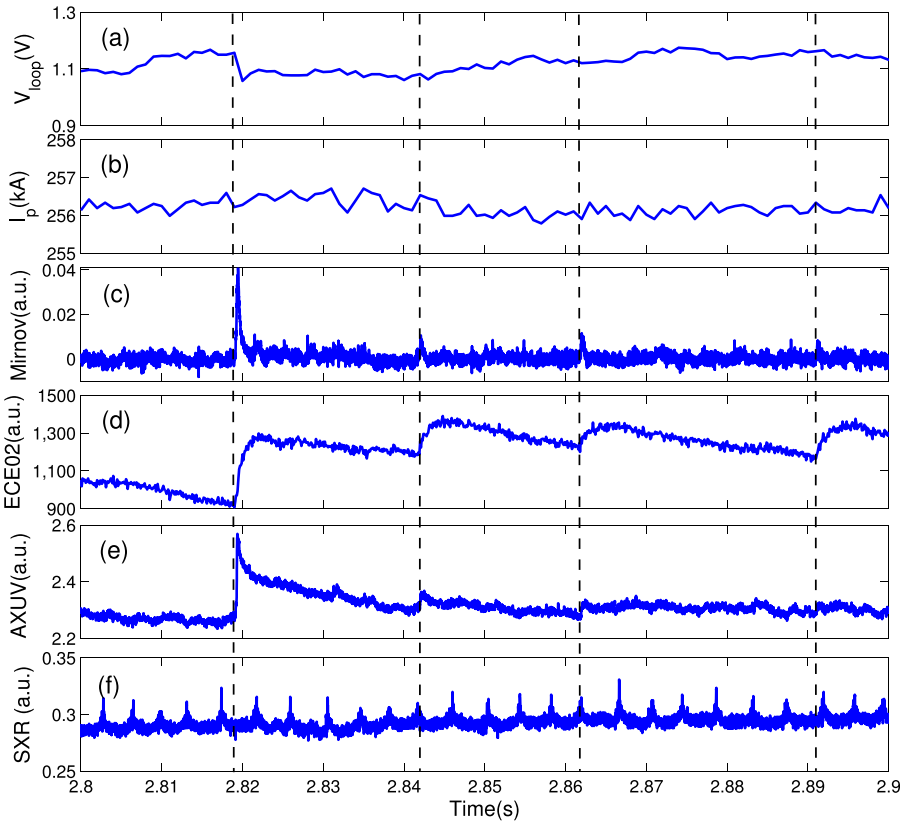

FIG. 2. Time evolution of the plasma parameters: (a) loop voltage V_{loop}, (b) plasma current I_p, (c) Mirnov signal, (d) non-thermal ECE (ECE02) signal, (e) AXUV photodiode signal, and (f) soft x-ray radiation (SXR).

The VB diagnostic system[11] measures the visible bremsstrahlung emission from plasma electrons. During shot #28957, strong spikes were observed in the VB signals from the plasma center during large MHD $m/n = 2/1$ spikes.

The absolute extreme ultraviolet (AXUV) photodiode signals represent the total radiated power from the plasma and allow radiated power measurements to be performed over a wide range of photon energies of $1\,\text{eV} < E_\gamma < 6000\,\text{eV}$. The AXUV and VB systems have the same temporal resolutions.

III. EXPERIMENTAL RESULTS

The stepwise increases in the non-thermal ECE signal were observed in the EAST runaway discharge #28957 (Ref. 7) when the MHD ($m/n = 2/1$) amplitude spikes emerged. Approximately every 0.2–0.3 s, rapid changes in the intensity and the synchrotron spot (transition from a hollow to a filled structure, see Fig. 3) occurred when the amplitudes of the MHD ($m/n = 2/1$) spikes and the ECE step-like jumps were stronger.[7] Now we describe these events in more detail.

Type I events: The MHD ($m/n = 2/1$) small amplitude spikes emerged approximately every 0.02 s and coincided with sawtooth $m/n = 1/1$ peaks in these cases (e.g., at $t \approx 2.84$ s, 2.86 s, and 2.89 s in Figs. 2(c) and 2(f)). During type I events, small step-like non-thermal ECE jumps were observed. These step-like ECE jumps coincided with the MHD ($m/n = 2/1$) small amplitude spikes (see Figs. 2(c) and 2(d)). Only a small correlation of the AXUV signals with these small MHD ($m/n = 2/1$) spikes (Fig. 2(e)) was observed. The asymmetrical ring-like IR spot from the runaways (hollow structure) did not change during the type I events.

Type II events: Huge MHD spikes emerged approximately every 0.5 s ($t \approx 2.82$ s in Fig. 2(c) and $t \approx 2.82$ s, 3.35 s, and 3.84 s in Fig. 4(c)), and in these cases they were not correlated with the sawtooth $m/n = 1/1$ peaks. The larger ECE jumps (Fig. 2(d) and Fig. 4(e)), the strong VB signal spikes (Figs. 4(f) and 4(g)), the strong spikes of the AXUV signals (Fig. 2(e); see, e.g., $t \approx 2.82$ s), and the strong hard x-ray (HXR) signal drops (Fig. 4(h)) were correlated with the huge MHD spikes. Practically, all channels of the VB diagnostic system showed strong spikes in these cases. During type II events, the change in the IR spot from a hollow structure to a filled structure occurred and these IR spot transitions were correlated with the MHD spikes (see Fig. 2 ($t \approx 2.82$ s) and Fig. 3).

Type III events: In comparison with type I events, larger amplitude MHD ($m/n = 2/1$) spikes were observed approximately every 0.3 s ($t \approx 3.1$ s, 3.6 s in Figure 4(c)) after each large (type II event) MHD spike. The MHD $m/n = 2/1$ spikes were not correlated with the sawtooth $m/n = 1/1$ peaks. The ECE jumps (Fig. 4(e)) and the HXR signal drops (Fig. 4(h)) were correlated with the MHD ($m/n = 2/1$) spikes, but only one channel of the VB diagnostic system showed small spikes. The change of the IR spot from a hollow structure to a filled structure was also observed.

The signal from the neutron detectors (photo-neutrons) did not change at all during these types I–III events. In EAST, this signal corresponds to runaways with energies in the 14–25 MeV range.

IV. DISCUSSION

In low density plasma ($n_e \sim 10^{19}\,\text{m}^{-3}$), the occurrence of runaway electrons is connected to their continuous

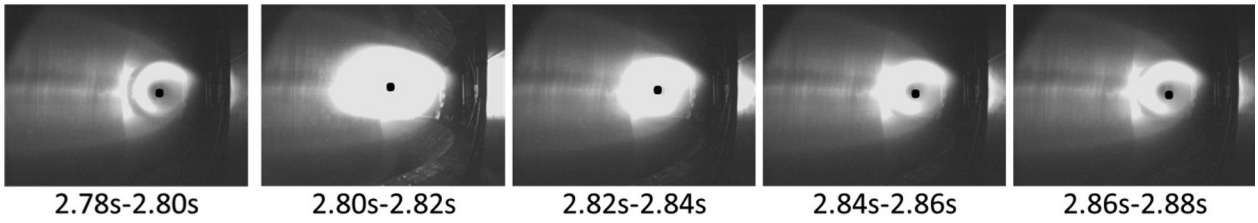

FIG. 3. Five continuous frames of images taken by the black and white camera from 2.78 s to 2.88 s. The position of pixel B is indicated by the black dot.

acceleration by the tokamak toroidal equilibrium electric field $E_{/\!/} \approx 0.1\,\mathrm{V/m}$. The runaway energy $E \approx 30\,\mathrm{MeV}$ was deduced from a joint analysis of the synchrotron radiation spectra and the synchrotron radiation spot shape in EAST discharge #28957.[7,9] This means that in EAST discharge #28957, the secondary runaway generation process should take place with avalanche time t_0[12–14]

$$t_0 \approx \sqrt{12} m_e c L (2 + Z_{eff})/9eE_{/\!/}. \tag{1}$$

Note that in the EAST case, the inequality $E_{/\!/} \gg E_{CH}$ holds, where $E_{CH} = e^3 n_e L/4\pi\varepsilon_0^2 m_e c^2$.[15] Here, e and m_e are the charge and the resting mass of the electron, L is the Coulomb logarithm, Z_{eff} is the effective ion charge number, and c is the velocity of light.

The inequality

$$p_\perp > p_{\perp,cr} \tag{2}$$

determines the runaway region for the secondary electrons[16,17] where

$$p_{\perp,cr} = \sqrt[4]{12}\,\mathrm{p}_{cr}(2 + \mathrm{Z}_{eff})^{0.5}/3, \quad p_{cr}^2 = e^3 m_e n_e L/4\pi\varepsilon_0^2 E_{/\!/}. \tag{3}$$

The inequality

$$p_{/\!/} > p_{/\!/,cr} \tag{4}$$

determines the runaway region of the primary (Dreicer) electron runaway generation process[18] where

$$p_{/\!/,cr} = p_{cr}(2 + Z_{eff})^{0.25}. \tag{5}$$

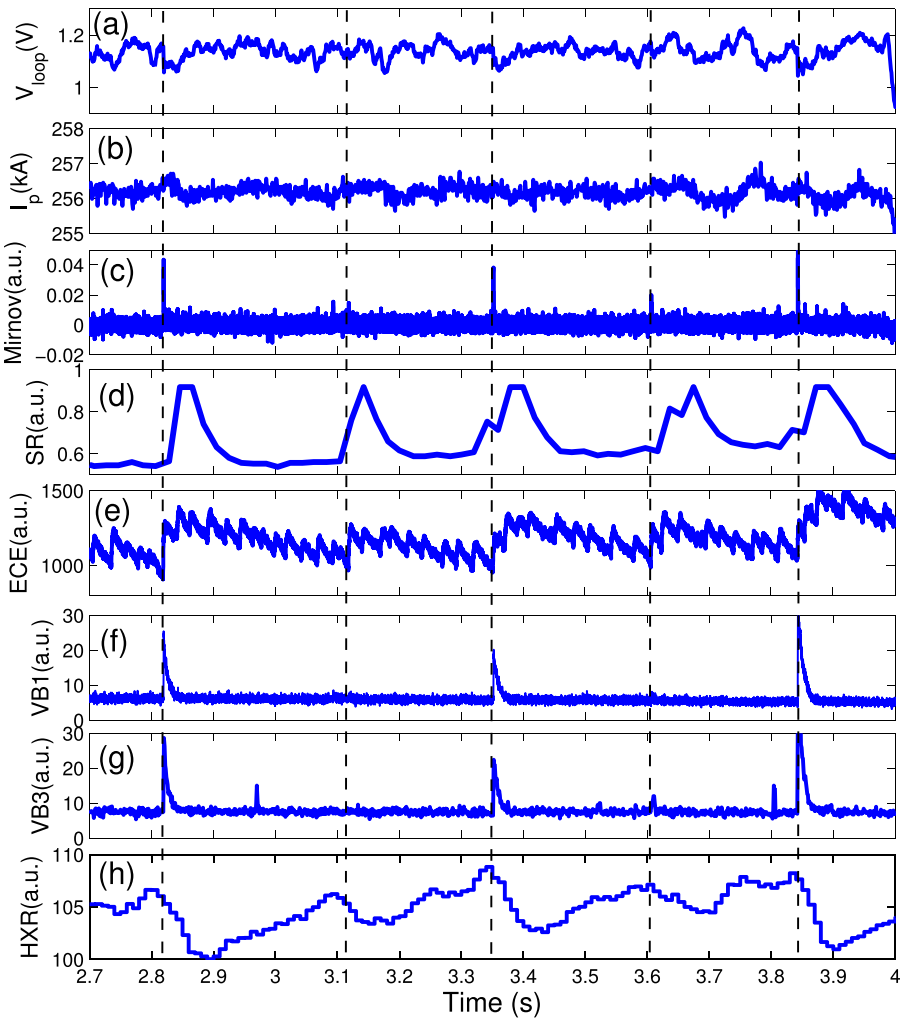

FIG. 4. Time evolution of the plasma parameters: (a) loop voltage V_{loop}, (b) plasma current I_{p}, (c) Mirnov signal, (d) local intensity of synchrotron radiation (SR) in pixel B, (e) non-thermal ECE (ECE02) signal, (f) VB1 signal, (g) VB3 signal, and (h) BGO scintillator detector signal (HXR).

The secondary runaway generation is strongly dependent on $Z_{\rm eff}$, whereas in the primary (Dreicer) runaway generation case, the dependence on $Z_{\rm eff}$ is much weaker.

As a result of the runaway generation processes, local changes in the plasma current density profile should occur (around the $q=2$ rational magnetic surface, where the runaway electrons are located). Recall here that the tearing mode stability depends rather sensitively on the current-density gradient in the vicinity of the resonant surface.[8] These local changes in the plasma current density profile near the $q=2$ rational magnetic surface may be the trigger for the strong enhancement of the MHD activity ($m/n=2/1$ spikes). Note that in Ref. 19, it was shown that the runaway electrons are better confined inside magnetic islands.

The generation of suprathermal electrons should be enhanced during these MHD spikes because of the fast changes in the magnetic flux (squeezing and reconnection of the magnetic field lines). Bursts of induced electric fields also occurred.[8] During these bursts of the induced electric field $E_{//}$, electron runaway regions (2) and (4) increased because the value of p_{cr} dropped (see Eq. (3)). The abrupt growth in the suprathermal electron population occurred during these bursts. Therefore, the step-like non-thermal ECE jumps may be explained by the abrupt growth in the suprathermal electron generation (number of runaways, not FPAS events) during MHD $m/n=2/1$ spikes. Enhancement of the secondary runaway generation process also occurred. Note here that the runaway electron secondary generation process is a non-local process in principle (see, e.g., Ref. 13). The integral of the close collisions relates the variations in the electron distribution function at the beginning of the runaway region (the suprathermal population of the runaways) to its values in the high energy region (30 MeV electron population).

In the presence of a tokamak toroidal equilibrium electric field, direct data separation with regard to the generation of suprathermal electrons caused by MHD activity is veiled. Nevertheless, the effect of the MHD modes on the generation of suprathermal electrons was demonstrated during T-10 tokamak experiments.[20,21]

Type I events: The non-thermal ECE signal is detected from the beginning of the runaway region. The generation of suprathermal electrons should be enhanced during the MHD spikes because of the fast change in the magnetic flux. An electric field was induced, and the suprathermal electrons are generated inside the current layer that is formed during the reconnection of the magnetic field where the electric field was induced.[8]

The step-like ECE jumps that occurred about every 0.02 s coincided with the MHD ($m/n=2/1$) small amplitude spikes when they coincided with sawtooth $m/n=1/1$ peaks (Figs. 2(c), 2(d), and 2(f)). Enhancement of the MHD plasma activity (spikes) acted as a trigger for the abrupt growth (bursts) of the suprathermal electron generation process. During small MHD $m/n=2/1$ spikes, only step-like jumps in the ECE signal were observed, while rapid changes in the synchrotron spot were not observed.

Types II–III events: From Eq. (1), we obtain the avalanching time $t_0 \approx 0.5$ s for the EAST parameters $E_{//} \approx 0.1$ V/m, $Z_{\rm eff} \approx 3$, $T_e(0) = 0.55$ keV, and $L \approx 15$. This avalanching time value $t_0 \approx 0.5$ s is of the same order as the value of the time of strong MHD activity (0.3 s or 0.5 s intervals). During this time (0.3 s or 0.5 s), as a result of strong runaway generation, stronger local changes in the current-density gradient should occur near the $q=2$ rational surface. These changes in plasma current density profile may act as the trigger for stronger enhancement of the MHD $m/n=2/1$ activity approximately every 0.3 s or 0.5 s.

Small increasing jump-drops in the $V_{\rm loop}$ signal and the plasma current $I_{\rm p}$ (correlated with huge MHD $m/n=2/1$ spikes) are visible in Figs. 2(a) and 2(b) for $t \approx 2.82$ s and in Figs. 4(a) and 4(b) for $t \approx 2.82$ s, 3.35 s, and 3.84 s. These increasing jump-drops in $V_{\rm loop}$ and $I_{\rm p}$ are evidence of the enhancement of the runaway generation process. Also, the enhancement of the MHD plasma activity ($m/n=2/1$ spikes) is again a trigger for abrupt growth in suprathermal electron generation and for rapid changes in the non-thermal ECE signal. Enhancement of the suprathermal electron generation process (near the $q=2$ rational surface) leads to enhancement of the secondary runaway generation process.

With regard to the rapid changes in the synchrotron spot (the transition of the IR spot from a hollow structure to a filled structure), we believe that the strong MHD $m/n=2/1$ spikes represent evidence of the fast reconnections of the magnetic field lines (as a result of resistive tearing modes or a collisionless mode) inside the larger plasma volume. The occurrence of a stochastic magnetic field region inside the larger central plasma volume leads to radial runaway beam spreading. Thus, the transition of the IR spot to a filled structure was caused by runaway beam radial spreading. The beam spreading time is approximately $\tau_{\rm D} \sim (\mu_0/\eta_{\rm eff})\Delta^2 \sim 15$ ms, where $\Delta \approx 8$ cm is the distance from the inner side of the runaway electron beam to pixel B (in Fig. 3, the position of pixel B is shown by a black dot). Here, $\eta_{\rm eff}$ is the effective resistivity (Eq. (4) in Ref. [7]). This time, $\tau_{\rm D}$ is less than the time resolution (20 ms) of the synchrotron radiation measurements shown in Fig. 3. Note that a change in the pitch angle may also occur because of the fast changes in the magnetic field line directions with respect to the runaway electron velocity directions during magnetic reconnections.

During bursts of the value of $E_{//}$, the suprathermal electron population increases. When these suprathermal electrons reach (through acceleration by $E_{//}$) the high energy region ($\sim$30 MeV), then the intensity of the synchrotron radiation in the pixel B position increases at specific times and then the SR signal drops (Fig. 4(d)). After bursts in the value of $E_{//}$, the ECE signal decreases because the suprathermal electron generation is also decreasing (the increase in p_{cr} and dilution of the runaway electron local density near the $q=2$ rational magnetic surface occurs as a result of beam spreading). Losses of suprathermal electrons also occur (compare with Fig. 7 in Ref. 21).

Therefore, the number of high energy runaway electrons is effectively limited. As a result, the runaway generation process is reduced during certain times. This is why the HXR signal drops after MHD $m/n=2/1$ spikes (Fig. 4(h)). Then, the HXR signal increases because of secondary

runaway generation until a new MHD $m/n = 2/1$ spike (roughly every 0.3 s or 0.5 s for types II–III events) occurs.

In Ref. 22, runaway electron microturbulence transport that was strongly decreasing $(1/E)$ for larger energies was shown. This may explain why the losses of the runaways with the high energies in the 14–25 MeV range were very small and why the neutron detector signal did not change at all.

The strong VB signal spikes (Figs. 4(f) and 4(g)) show fast changes in the behavior of their impurities during intense MHD $m/n = 2/1$ spikes. The spikes (#28957) at the AXUV detectors were associated with the non-thermal electrons because the AXUV detectors show abrupt enhancement of the radiation produced by radiative scattering and excitation of the background plasma and impurities during the bursts of the non-thermal electrons. This may change the local value of Z_{eff}. Therefore, a fast change in the secondary runaway electron generation avalanching time t_0 (compared with that of Ref. 13) may also take place (see the negative spikes in the synchrotron radiation intensity, Fig. 4(d)).

In Ref. 23, the FPAS event was explained by the interaction between the runaway electrons with lower hybrid waves (LHW) via anomalous Doppler broadening. Note that no LHWs were injected into plasma, and that there is no evidence of LHW excitation in the discharge #28957. There will not be interactions between the runaway electrons and the LHW.

V. CONCLUSIONS

In the EAST runaway discharge, stepwise increases in the non-thermal ECE signal coincided with the enhancement of the MHD activity that was a peculiarity of this particular shot. The runaway energy $E \approx 30$ MeV was deduced from EAST runaway discharge #28957, under conditions where the secondary runaway generation process should take place. The runaways were located around the $q = 2$ rational magnetic surface and the runaway current was not small. In experiment presented here, the effects of the magnetic reconnections on the runaway generation and the MHD plasma activity were shown. Our main conclusions are as follows.

As a result of local runaway electron generation, local changes in the current-density gradient near $q \approx 2$ should occur. These changes in the plasma current density profile may be the trigger for the enhancement of the MHD $m/n = 2/1$ activity. The MHD $m/n = 2/1$ spikes acted as a trigger for the enhancement of additional suprathermal electron generation (bursts) during magnetic reconnections. The step-like jumps in the non-thermal ECE signal were indirect indications of the bursts of the suprathermal electrons (during MHD $m/n = 2/1$ spikes). The jump-drops in the V_{loop} signal and the increasing I_{pl} provided evidence of the enhancement of the runaway generation process during strong MHD $m/n = 2/1$ spikes.

The stochastic magnetic field region appeared during MHD activity. When the MHD $m/n = 2/1$ spikes were not too large, the stochastic magnetic field region was small. No large-scale radial spreading of the runaway beam was observed (i.e., no changes in the synchrotron spot). During huge MHD $m/n = 2/1$ spikes, a large stochastic magnetic field region occurred. The local runaway electron density dropped near the $q = 2$ rational magnetic surface, where the runaway beam generation was stronger. Secondary runaway generation was therefore reduced during certain times and the number of high energy runaways was effectively limited (the HXR signal behavior indicated this process). Rapid changes in the synchrotron spot from a hollow structure to a filled structure were the result of changes in the runaway beam structure caused by runaway radial spreading. The AXUV and VB signal spikes during strong MHD $m/n = 2/1$ activity were also associated with the suprathermal electron bursts.

All experimental signals presented here were correlated with each other and they provided an indirect indication of our main conclusion that the step-like non-thermal ECE jumps were connected to the abrupt growth in suprathermal electrons induced by the bursting electric fields at the reconnection events that occur during MHD plasma activity. While the present EAST runaway experiment cannot provide full data for quantitative analysis of the rapid changes in the synchrotron spot and its intensity and of the stepwise increases in the non-thermal ECE, the results presented here have contributed to an essential new interpretation of this intriguing phenomenon.

In addition to Dreicer and avalanching runaway generation, other mechanisms may also play important roles in runaway generation, especially in ITER. For example, these mechanisms include the hot tail mechanism, and the gamma mechanism (see, e.g., Ref. 24). Our results may also be one of those mechanisms. For example, the magnetic behavior during plasma disruption is always complex. The abrupt growth of suprathermal electrons induced by bursting electric fields at the reconnection events may potentially be seed runaways that can cause avalanching growth of the number of runaways.

ACKNOWLEDGMENTS

The work of R. J. Zhou and L. Q. Hu was supported by the National Nature Science Foundation of China under Grant No. 11405219 and was partially supported by the JSPS-NRF-NSFC A3 Foresight Program in the field of Plasma Physics (NSFC No. 11261140328).

[1]ITER Physics Expert Group on Disruptions, Plasma Control, and MHD and ITER Physics Basis Editors, "Chapter 3: MHD stability, operational limits and disruptions," Nucl. Fusion **39**, 2175 (1999).
[2]T. C. Hender *et al.*, "Chapter 3: MHD stability, operational limits and disruptions," Nucl. Fusion **47**, S128 (2007).
[3]H. Dreicer, Phys. Rev. **115**, 238 (1959).
[4]Yu. A. Sokolov, JETP Lett. **29**, 218 (1979).
[5]R. Jaspers, "Relativistic runaway electrons in tokamak plasmas," Ph.D. thesis (Eindhoven University of Technology, The Netherlands, 1995), see http://repository.tue.nl/431410.
[6]I. Entrop, "Confinement of relativistic runaway electrons in tokamak plasmas," Ph.D. thesis (Eindhoven University of Technology, The Netherlands, 1999), see http://repository.tue.nl/528445.
[7]R. J. Zhou, L. Q. Hu, E. Z. Li, M. Xu, G. Q. Zhong, L. Q. Xu, S. Y. Lin, J. Z. Zhang, and the EAST Team, Plasma Phys. Controlled Fusion **55**, 055006 (2013).
[8]D. Biskamp, *Magnetic Reconnection in Plasmas* (Cambridge University Press, Cambridge, 2000).

[9]R. J. Zhou, I. M. Pankratov, L. Q. Hu, M. Xu, and J. H. Yang, Phys. Plasmas **21**, 063302 (2014).
[10]Y. Shi, J. Fu, H. Gao, F. Wang, J. Li, Y. Yang, Z. Chen, B. Wan, and EAST Team, Rev. Sci. Instrum. **81**, 033506 (2010).
[11]Y. Chen, Z. Wu, W. Gao, L. Zhang, Y. Jie, J. Zhang, Q. Zang, J. Huang, G. Zuo, and J. Zhao, Plasma Phys. Controlled Fusion **56**, 105006 (2014).
[12]I. M. Pankratov and N. T. Besedin, "Runaway electron secondary generation," in *Proceedings of 23nd EPS Conference on Controlled Fusion and Plasma Physics, Kiev, 1996* (European Physical Society, 1996), Vol. 20C, part I, p. 279.
[13]I. M. Pankratov, R. Jaspers, K. H. Finken, I. Entrop, and G. Mank, Nucl. Fusion **38**, 279 (1998).
[14]R. D. Gill, B. Alper, M. de Baar, T. C. Hender, M. F. Johnson, and V. Riccardo, Nucl. Fusion **42**, 1039 (2002).
[15]J. W. Connor and R. J. Hastie, Nucl. Fusion **15**, 415 (1975).
[16]N. T. Besedin and I. M. Pankratov, Nucl. Fusion **26**, 807 (1986).
[17]I. M. Pankratov, R. Jaspers, K. H. Finken, and I. Entrop, "Secondary generation of runaway electrons and its detection in tokamaks," in *Proceedings of 26th EPS Conference on Controlled Fusion and Plasma Physics, Maastricht, 1999* (European Physical Society, 1999), Vol. 23J, p. 597.
[18]V. Fuchs, R. A. Cairns, C. N. Lashmore-Davies, and M. M. Shoucri, Phys. Fluids **29**, 2931 (1986).
[19]I. Entrop, R. Jaspers, N. J. Lopes Cardozo, and K. H. Finken, Plasma Phys. Controlled Fusion **41**, 377 (1999).
[20]P. V. Savrukhin, Phys. Plasmas **9**, 3421 (2002).
[21]P. V. Savrukhin and E. A. Shestakov, Nucl. Fusion **55**, 043016 (2015).
[22]T. Hauff and F. Jenko, Phys. Plasmas **16**, 102308 (2009).
[23]J. R. Martin-Solis, R. Sanchez, and B. Esposito, Phys. Plasma **9**, 1667 (2002).
[24]H. M. Smith and E. Verwichte, Phys. Plasmas **15**, 072502 (2008).